Synlett M. Lange et al. THIEME OPEN ACCESS Cluster

London Dispersion-Assisted Low-Temperature Gas Phase Synthesis of Hydrogen Bond-Inserted Complexes

Manuel Lange
Elisabeth Sennert
Martin A. Suhm*

Institut für Physikalische Chemie, Georg-August-Universität Göttingen, Tammannstr. 6, 37077 Göttingen, Germany
msuhm@gwdg.de

Published as part of the Cluster
Dispersion Effects

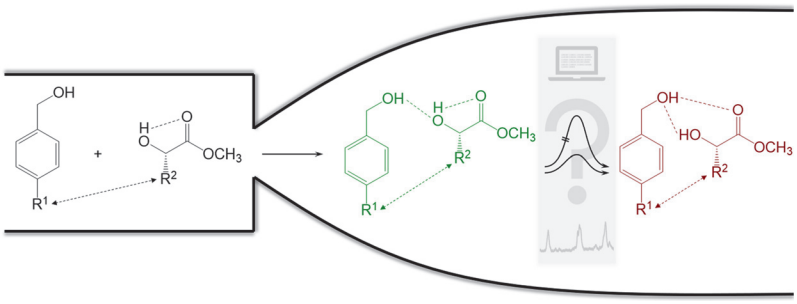

Received: 02.09.2022
Accepted after revision: 20.10.2022
Published online: 23.11.2022 (Version of Record)
DOI: 10.1055/s-0042-1751385; Art ID: ST-2022-09-0390-C

Abstract Supersonic expansions of organic molecules in helium carrier gas mixtures are used to synthesize model (pre)reactive complexes at low temperature. Whether or not barriers for hydrogen bond rearrangements can be overcome in this collisional process is not well understood. Using the example of alcohols inserting into intramolecular hydrogen bonds of α-hydroxy esters, we explore whether dispersion energy donors can assist the process in a systematic way. Bromo, iodo, and *tert*-butyl substitution of benzyl alcohol in the *para*-position is used to show that the insertion process into methyl glycolate is controllable, whereas it is largely avoided for the chiral methyl lactate homologue. Methyl lactate appears to steer the transient chirality of benzyl alcohol derivatives in a uniform direction relative to the lactate handedness for the OH···O=C insertion product, as well as for the competing attachment to the hydroxy group of the ester. A simple rule based on the total binding energy in relation to the rearrangement barrier is tentatively proposed to estimate whether the insertion is feasible or not in such molecular complexes during expansion.

Key words spectroscopy, chirality induction, gas phase reaction, hydrogen bond topology, halogenation, α-hydroxy esters

At room temperature, weak intramolecular hydrogen bonds are easily overcome by thermal motion and cannot serve as kinetic barriers for the outcome of a molecular attachment reaction. This is different for the synthesis of molecular aggregates in supersonic jet expansions,[1] and even more so in helium nanodroplets,[2] where relatively low barriers of the order of a few kJ·mol^{-1} can effectively block reaction channels and lead to metastable cluster structures. One aspect that has not been systematically addressed in this area of research is the role of the aggregation energy that is released when the reaction partners meet in the gas phase and which remains in the collision complex until it is carried away by further collisions with the atoms of the carrier gas. In contrast to directional hydrogen bonds, London dispersion interactions add to this aggregation energy in a less specific and fairly universal way, making more energy available for any rearrangement within the complex.[3] Therefore, one may speculate that given enough dispersion energy, isomerization barriers of increasing size might be overcome and could give way to the global minimum structure hidden behind such barriers. The stickiness of London dispersion would thus give the collisional complex enough time and energy to overcome a sizeable barrier due to intramolecular hydrogen bonding.

To modify the cohesion between the gas phase reaction partners, two established strategies are explored in the present work. One is the popular replacement of hydrogen atoms by *tert*-butyl groups;[4] the other involves exchange with various halogen atoms. Moving down the periodic table in the halogen group is a frequent exercise in chemistry, with diverse outcomes due to counteracting trends. For the van der Waals complexes of hydrogen halides with argon, the structural preference (head or tail) switches between Br and I.[5] Halogen bonding to the N end of HCN becomes increasingly competitive with hydrogen bonding on increasing the size of the halogen.[6] In aqueous solution, methyl halides have an increasing affinity toward porphyrins and other hosts.[7] In axial–equatorial equilibria of halogenated cyclohexanes, steric and London dispersion contributions compete with each other.[8] Many other examples could be added.

In this work, we show that substituted benzyl alcohols indeed insert into the intramolecular hydrogen bond of α-hydroxy esters in the gas phase,[9] if this insertion leads to a lower-energy structure than does a barrierless attachment. Counter to previous expectations,[1] this may even be the case if the barrier from the cold complex with the attached alcohol to the inserted complex exceeds 10 kJ·mol^{-1}.

Whether the barrier is transmissive or not might depend on the transiently released cohesion energy of the complex. Both the driving force and the barrier height are modulated by *para*-substitution of the benzyl alcohol with a Br, I, or *tert*-butyl group. This is because the insertion channel moves the ester away from the *para*-substitution site.[10] By adding a methyl group in the α-position of the ester, the insertion product can be further destabilized and the transiently chiral benzyl alcohol is driven into a uniform enantiomeric conformation relative to the now chiral hydroxy ester. These theoretical predictions are shown to be consistent with experimental findings. Only a systematic study of several examples can disentangle the uncertainties in theoretical driving force and chirality induction predictions and the experimental evidence for insertion and chirality preference. The results might also be relevant for prereactive complexes at more typical reaction temperatures if correspondingly larger barriers maintain kinetic control.

The experimental and quantum-chemical procedures employed in this work closely follow the initial investigation of the parent benzyl alcohol and its *para*-chlorinated derivative in combination with the simplest achiral and chiral α-hydroxy esters.[10] We refer to that work for the details of the supersonic jet infrared and Raman spectroscopy techniques, and to the Supporting Information (SI) for the actual spectra obtained and for their assignment (see Figures S5–S8 for the spectra, Tables S8–S11 for the assigned band positions, and Table S12 for the experimental conditions), which is based on systematic harmonic shift predictions obtained at the B3LYP-D3(BJ)/def2-TZVP level[11,12] with the *ORCA 4.0* program suite.[13] The experimental outcome is analyzed in terms of optimized transition states and reaction paths acquired with the *Turbomole 7.3* package.[14] Applied ORCA and Turbomole parameters are listed in Tables S1 and S2 of the SI. Here, we focus on the correlation of the experimental yield with the theoretical barrier and with low-temperature exothermicity predictions. The co-aggregated species are abbreviated G for methyl glycolate, L for methyl lactate, and B for benzyl alcohol. Generic *para*-halogenation of B is abbreviated H, and specific halogenation is indicated by the corresponding element symbol (Cl, Br, I). *p*-(*tert*-Butyl)benzyl alcohol is abbreviated T, and the previously investigated methanol is abbreviated as M[15] (see Figure 1 for an overview of the structures, full names, and abbreviations of the aromatic alcohols and esters). An 'a' is added for the attachment product and an 'i' for the insertion product. If the transient axial chirality of the (substituted) benzyl alcohol has the same sign as the methyl lactate standard optical rotation [i.e., *g*– and *S*-(–)-lactate or *g*+ and *R*-(+)-lactate], we arbitrarily call the complex 'homochiral' (hom); otherwise, it is denoted 'heterochiral' (het). hom-ILi would thus be the inserted isomer of the (*G*-*g*-) 1:1 *p*-iodobenzyl alcohol with *S*-(–)-methyl lactate.

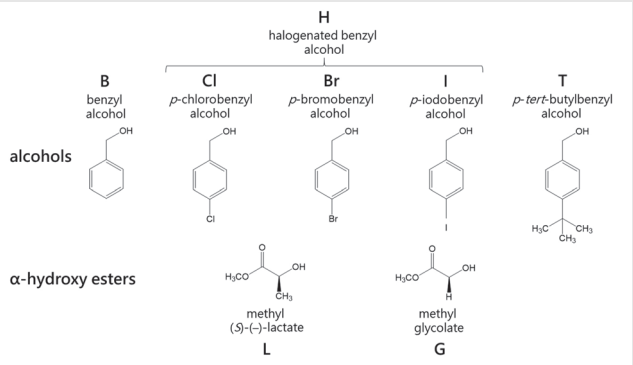

Figure 1 Structures, full names, and abbreviations of the aromatic alcohols and α-hydroxy esters investigated in this work.

The outcomes of the experiments are concisely summarized in Figure 2 for methyl glycolate and in Figure 3 for methyl lactate, and they are combined with the key energetic predictions at the B3LYP-D3(BJ)/def2-TZVP level, namely the zero-point energy-corrected relative energies of the insertion product (red) and the attachment product (green, normalized to zero), as well as the reaction barrier from the attachment perspective.

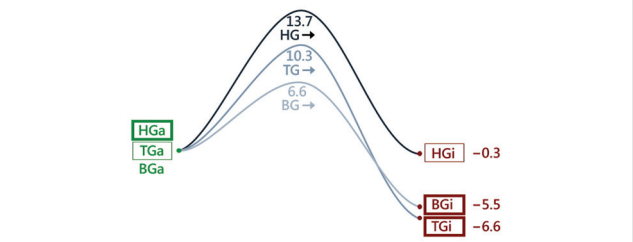

Figure 2 Computed (B3LYP-D3(BJ)/def2-TZVP) 0 K insertion barriers and relative energies in kJ·mol^{-1} from attachment (a) complexes of alcohols B, T, and H with G to the corresponding insertion complexes (i). For transmissive barriers (→), insertion dominates (heavy red frame) in the experiment; otherwise, it is detected as a trace product (⊣, thin frame, HGi). Attachment complexes dominate (HGa), survive as a trace (TGa), or are not detected (BGa). See the text for further explanations.

Heavy frames drawn around the complex labels indicate major products and light frames indicate minor products of the supersonic jet synthesis. The omission of a frame around the species means that this isomer was not detected. The quantification is carried out through predicted IR and Raman cross-sections.[10] When the energy calculations were repeated with the def2-QZVP basis set,[12] the relative energies of minima and connecting transition states changed by less than 0.6 kJ·mol^{-1} and the energies for dissociation into benzyl alcohol and hydroxy ester units (discussed later) rather uniformly dropped by less than 10% (see SI, Tables S6 and S7). This does not affect the conclusions of this work, and we continue with the consistent B3LYP-D3(BJ)/def2-TZVP approach for optimized structures, electronic energies, harmonic zero-point corrections,

and OH stretching wavenumbers. As shown before,[10] DLPNO-CCSD(T)/aug-cc-pVQZ[16] calculations also do not change the energetic picture significantly, but they tend to stabilize the attachment complexes by 1 to 3 kJ·mol^{-1} (see SI, Tables S4 and S5).

For the glycolate case, it has previously been shown that B quantitatively inserts into the hydrogen bond over a low barrier with a strong driving force.[10] T is predicted to increase the barrier substantially and to enhance the driving force slightly. We found that this leaves a trace of attachment product TGa, but TGi is the dominant product. Thus, the barrier starts to have some influence. Halogenation (quite independent of whether it is Cl[10] or now Br or I; see SI, Figure S2) further increases the barrier and essentially removes the driving force. This still allows for a trace of the insertion product HGi, but the main product is now HGa. Depending on the accuracy of the calculations, this observation can either be interpreted as kinetic hindrance (the barrier of nearly 14 kJ·mol^{-1} becoming limiting) or an insufficient driving force.

On switching from methyl glycolate to methyl lactate, the OH group becomes a better hydrogen bond acceptor and, therefore, the attachment to it becomes more attractive, whereas insertion into the intramolecular hydrogen bond does not profit as much. For BL, the previous finding was that insertion is hindered but not completely avoided,[10] either due to a higher barrier or a reduced driving force. Chlorination further increases the barrier and eliminates the driving force, thereby completely suppressing insertion. This is confirmed here for Br and I substitution (see SI, Figure S3). Therefore, no HLi is detected along with HLa. The effect of T is again to somewhat increase the barrier relative to B, while conserving the reduced driving force. Experimentally, a small amount of TLi is observed. Therefore, a barrier of more than 13 kJ·mol^{-1} does not completely prevent insertion. TLa is now the dominant, but not the exclusive, product. Even if the calculations underestimate the driving force, insertion over such a barrier is quite notable and calls for a mechanistic extension of previous findings for smaller aggregates.[1]

A remarkable theoretical prediction for the chiral lactate, which is consistent with the lack of experimental evidence for coexisting homo- and heterochiral products with all benzyl alcohol derivatives, is the prediction of a systematic homochiral energy preference. The lactate directs the incoming benzyl alcohol into a uniform helicity (which is composed of two torsional angles CC–CO (*G*) and CO–OH (*g*) of the same sign[17]), regardless of whether it just attaches to or inserts into the intramolecular hydrogen bond. The insertion case is easy to understand because the heterochiral combination places the extra methyl group between the plane of the aromatic ring and the hydroxy ester plane and reduces their London dispersion attraction. This het destabilization is particularly pronounced for TL. If the chirality induction were not quantitative, it would give rise to doublets in the relevant IR and Raman spectra, which should frequently exceed the spectral resolution. Although spectral congestion and coincidental overlap prevent an unambiguous statement, the fact that such splittings are not observed for B, Cl, Br, I, and T strengthens the hypothesis that the predicted chirality induction is indeed active in the supersonic jet experiment.

The experimental barrier-crossing success can be compared with the calculated barrier height and the energy that is internally released when the alcohol docks onto the OH group of the hydroxy ester to form an attached complex (Figure 4). The zero-point corrected binding energies of the complexes relative to the most stable monomer conformations are listed in Table S3 of the SI. If only 25% of that energy is used to cross the barrier, it is possible to rationalize why inserted complexes dominate the jet expansion for BG

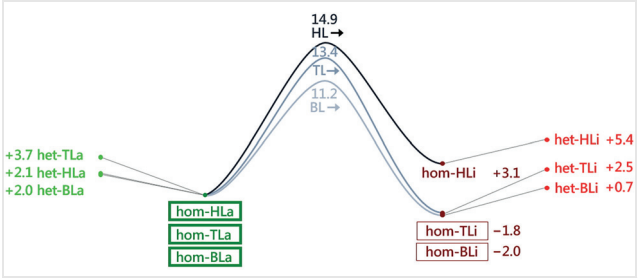

Figure 3 Computed (B3LYP-D3(BJ)/def2-TZVP) 0 K insertion barriers and relative energies in kJ·mol^{-1} from transiently homochiral attachment (a) complexes of alcohols B, T, and H with L to the corresponding insertion complexes (i). Insertion is at best detected as a byproduct (thin red frame) in the experiment. Lines connect the homochiral complexes to the energy of their metastable heterochiral counterparts. See the text for further explanations.

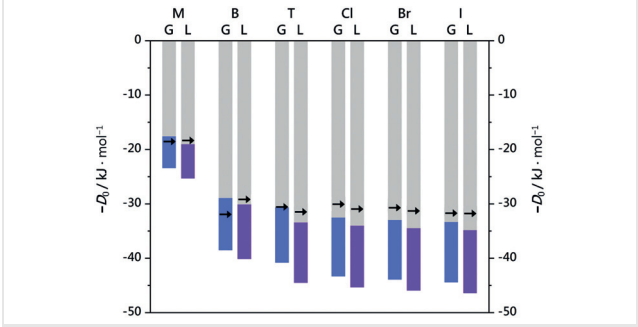

Figure 4 Comparison of the binding or negative dissociation energy $-D_0$ released when the alcohols M, B, T, Cl, Br, and I attach to the hydroxy esters G and L (full bars), and one quarter of it (colored bar sections), with transmissive (→) and blocking (⊣) barrier heights for insertion. All values are computed at the B3LYP-D3(BJ)/def2-TZVP level and include a harmonic zero-point correction. For M, the barriers are so low that transmission is granted (see SI, Figure S4). For the heavier systems, it is observed that transmission to a downhill insertion complex is dominant when the barrier does not exceed about one quarter of D_0.

and TG, whereas the halogenated glycolate complex HG and all lactate complexes would need more than 25% of the attachment energy to insert. In those cases where trace amounts of insertion were still detected, the fraction is around 30% and the process is predicted to be at least slightly exothermic. It was shown that even for the unsubstituted systems, London dispersion typically accounts for 75% or more of the total interaction energy for the attachment products.[10] Furthermore, *para*-chlorination at the benzyl alcohol was shown to lead to a significant enhancement of the dispersion interactions in the attachment process. The energy freed upon attachment can thus be modified by substitution, but this also affects the barrier to insertion, because the inserted complex removes the close interaction of the ester with the *para*-position of the benzyl alcohol. The comparison of a fraction of the binding energy of the attachment complex (empirically 25% in the present systems) with the unimolecular barrier to be overcome for insertion is a plausible approach, given that the density of states at this energy and the statistical reaction rate at the barrier threshold will be very slow. It has to be accelerated by substantial excess energy to be relevant on the microsecond timescale of supersonic expansions. However, this cannot be more than a rough and tentative rule of thumb that requires further evidence.

Because most of the conclusions have been derived from experiments in combination with harmonic B3LYP-D3(BJ)/def2-TZVP predictions, it is advisable to analyze higher-level DLPNO-CCSD(T)/aug-cc-pVQZ energy calculations at the B3LYP-D3(BJ)/def2-TZVP-optimized minimum structures, including an analysis of the London dispersion part of the interaction energy between the fragments. Figure 5 shows the computed substitution dependence of the insertion preference over attachment (black) and the dispersion energy contribution to this preference, through the interaction energy difference of the fragments (red, LED scheme)[18] for G and L complexes. Because the total energy includes deformation energy whereas the interaction energy does not do so, the trends in the curves are more significant than the absolute values.[10]

The black curves show that the extra methyl group in L systematically destabilizes insertion over attachment, largely by increasing the hydrogen bond-accepting capability of the OH group. They also show that halogenation destabilizes insertion for G and L, and that this preference is almost the same for het (dashed, species not observed in experiment, because they are less stable independent on attachment or insertion) and hom pairings for L.

This parallel behavior of het and hom pairs is actually the consequence of a cancellation effect, as shown by the dispersion contribution to the preference (in red). For G, the black and red curves run closely parallel, so that any London dispersion preference for insertion is reflected in the total energy difference (black). For L, the red curve runs much

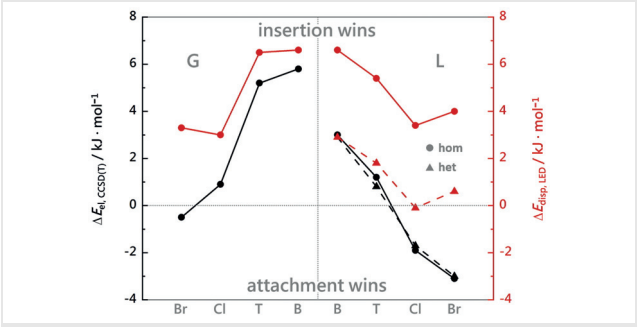

Figure 5 DLPNO-CCSD(T)/aug-cc-pVQZ energy differences between insertion and attachment at the B3LYP-D3(BJ)/def2-TZVP-optimized 1:1 complex structures. The lines connect different substitutions at the *para*-position of the benzyl alcohol. Dashed lines show the values for het pairings in the case of L. The London dispersion contribution to the interaction energy difference (LED scheme) is plotted in red and the total electronic energy is plotted in black. See the text for further explanations.

higher in the hom case, where the two molecular planes can align well with each other in the insertion complex. This dispersion advantage is evidently counteracted by other contributions, such as repulsion. In the het case, the chirality-generating methyl group prevents an alignment of the planes, and thus the dispersion advantage of insertion is lost to a large degree. Because this also reduces repulsive forces, the overall insertion preference for het pairs is similar to that for hom pairs, despite the large hom preference for dispersion.

Another interesting detail is seen when comparing Cl with Br. While the total energy indicates more attachment preference for Br, the dispersion contribution uniformly suggests less attachment preference for Br. It will be interesting to see how this divergence between the London dispersion contribution and the total energy develops for I.

The following qualitative picture is thus proposed: during the formation process of the attachment complexes in the early stage of the expansion, some of the aggregation energy is removed by carrier gas collisions to stabilize the aggregate. The remaining excess energy is needed to drive the isomerization reaction over the barrier, before it is carried away by further strong collisions or it is transferred to a slow carrier gas atom during the exothermic insertion.[3,19] In any case the rule[1] that supersonic relaxation is hindered by barriers of more than about 5 kJ·mol^{-1} has to be adapted for the aggregation of larger molecules, particularly when combined with a downhill process.

Whether or not it is possible to derive a general low-temperature gas phase synthesis principle in which reaction barriers can be overcome by adding dispersion-energy donors to the reactants[20] remains to be seen. With appropriate placing, these auxiliary substituents might even be able to open specific reaction channels preferentially. For true reactions, it would, however, be necessary to mix the

reactants in or immediately after the nozzle, because otherwise the reaction might already proceed nonspecifically in the stagnation chamber before the nozzle.

There is one caveat for the insertion process of benzyl alcohol derivatives into α-hydroxy esters, which requires future computational investigation. We have so far assumed that isomerization proceeds directly from the (hot) attached isomer to the inserted isomer, because these are the species that are detected spectroscopically. It is conceivable that insertion preferentially exploits a lower barrier from another isomer of the 1:1 complex that is transiently formed near the nozzle. A systematic investigation of the network of transition states between the local minima in such alcohol/hydroxy ester complexes is currently underway.[21] Also, it would be helpful to structurally investigate some of the discussed complexes by rotational spectroscopy,[22] to further verify the validity of the computational approaches and the propensity toward different isomers. Finally, extensions of this analysis to other hydroxy compounds, such as achiral phenols[23] or permanently chiral aromatic alcohols,[24] would be of interest.

Conflict of Interest

The authors declare no conflict of interest.

Funding Information

This work was funded by the Deutsche Forschungsgemeinschaft (DFG, German Research Foundation)-271107160/SPP1807 (ML, dispersion effects), 389479699/RTG2455 (ES, halogenation effects, benchmarking of reaction barriers and hydrogen bond energies) and 405832858 (computer cluster).

Acknowledgment

We thank the mechanics and electronics workshops for the construction and maintenance of the jet expansion setups.

Supporting Information

Supporting information for this article is available online at https://doi.org/10.1055/s-0042-1751385.

References

(1) Ruoff, R. S.; Klots, T. D.; Emilsson, T.; Gutowsky, H. S. *J. Chem. Phys.* **1990**, *93*, 3142.
(2) Meyer, K. A. E.; Davies, J. A.; Ellis, A. M. *Phys. Chem. Chem. Phys.* **2020**, *22*, 9637.
(3) Erlekam, U.; Frankowski, M.; von Helden, G.; Meijer, G. *Phys. Chem. Chem. Phys.* **2007**, *9*, 3786.
(4) Rösel, S.; Balestrieri, C.; Schreiner, P. R. *Chem. Sci.* **2017**, *8*, 405.
(5) McIntosh, A.; Wang, Z.; Castillo-Chará, J.; Lucchese, R. R.; Bevan, J. W.; Suenram, R. D.; Legon, A. C. *J. Chem. Phys.* **1999**, *111*, 5764.
(6) Perkins, M. A.; Tschumper, G. S. *J. Phys. Chem. A* **2022**, *126*, 3688.
(7) Schneider, H.-J. *Acc. Chem. Res.* **2015**, *48*, 1815.
(8) Solel, E.; Ruth, M.; Schreiner, P. R. *J. Org. Chem.* **2021**, *86*, 7701.
(9) Katsyuba, S. A.; Spicher, S.; Gerasimova, T. P.; Grimme, S. *J. Chem. Phys.* **2021**, *155*, 24507.
(10) Lange, M.; Sennert, E.; Suhm, M. A. *Symmetry* **2022**, *14*, 357.
(11) (a) Grimme, S.; Antony, J.; Ehrlich, S.; Krieg, H. *J. Chem. Phys.* **2010**, *132*, 154104. (b) Lee, C.; Yang, W.; Parr, R. G. *Phys. Rev. B* **1988**, *37*, 785. (c) Becke, A. D. *J. Chem. Phys.* **1993**, *98*, 5648. (d) Becke, A. D. *Phys. Rev. A* **1988**, *38*, 3098. (e) Grimme, S.; Ehrlich, S.; Goerigk, L. *J. Comput. Chem.* **2011**, *32*, 1456.
(12) Weigend, F.; Ahlrichs, R. *Phys. Chem. Chem. Phys.* **2005**, *7*, 3297.
(13) Neese, F. *Wiley Interdiscip. Rev.: Comput. Mol. Sci.* **2018**, *8*, e1327.
(14) (a) Furche, F.; Ahlrichs, R.; Hättig, C.; Klopper, W.; Sierka, M.; Weigend, F. *Wiley Interdiscip. Rev.: Comput. Mol. Sci.* **2014**, *4*, 91. (b) *TURBOMOLE V7.3*; TURBOMOLE GmbH: Karlsruhe, **2018**, available from http//www.turbomole.com.
(15) Borho, N.; Suhm, M. A.; Le Barbu-Debus, K.; Zehnacker, A. *Phys. Chem. Chem. Phys.* **2006**, *8*, 4449.
(16) (a) Riplinger, C.; Sandhoefer, B.; Hansen, A.; Neese, F. *J. Chem. Phys.* **2013**, *139*, 134101. (b) Kendall, R. A.; Dunning, T. H. Jr.; Harrison, R. J. *J. Chem. Phys.* **1992**, *96*, 6796. (c) Woon, D. E.; Dunning, T. H. Jr. *J. Chem. Phys.* **1993**, *98*, 1358. (d) Wilson, A. K.; Woon, D. E.; Peterson, K. A.; Dunning, T. H. Jr. *J. Chem. Phys.* **1999**, *110*, 7667.
(17) Medel, R.; Suhm, M. A. *Phys. Chem. Chem. Phys.* **2020**, *22*, 25538.
(18) (a) Altun, A.; Neese, F.; Bistoni, G. *Beilstein J. Org. Chem.* **2018**, *14*, 919. (b) Schneider, W. B.; Bistoni, G.; Sparta, M.; Saitow, M.; Riplinger, C.; Auer, A. A.; Neese, F. *J. Chem. Theory Comput.* **2016**, *12*, 4778.
(19) Sohn, W. Y.; Kim, M.; Kim, S.-S.; Park, Y. D.; Kang, H. *Phys. Chem. Chem. Phys.* **2011**, *13*, 7037.
(20) Wagner, J. P.; Schreiner, P. R. *Angew. Chem. Int. Ed.* **2015**, *54*, 12274.
(21) Hein-Janke, B.; Mata, R. A. **2022**, personal communication.
(22) Medel, R.; Camiruaga, A.; Saragi, R. T.; Pinacho, P.; Pérez, C.; Schnell, M.; Lesarri, A.; Suhm, M. A.; Fernández, J. A. *Phys. Chem. Chem. Phys.* **2021**, *23*, 23610.
(23) Hong, A.; Moon, C. J.; Jang, H.; Min, A.; Choi, M. Y.; Heo, J.; Kim, N. J. *J. Phys. Chem. Lett.* **2018**, *9*, 476.
(24) (a) Scuderi, D.; Le Barbu-Debus, K.; Zehnacker, A. *Phys. Chem. Chem. Phys.* **2011**, *13*, 17916. (b) Seurre, N.; Le Barbu-Debus, K.; Lahmani, F.; Zehnacker, A.; Borho, N.; Suhm, M. A. *Phys. Chem. Chem. Phys.* **2006**, *8*, 1007.